Polypyrrole nanoparticles as a thermal transducer of NIR radiation in hot-melt adhesives

Fugang Li,[a] Mitchell A. Winnik,*[a] Anna Matvienko[b] and Andreas Mandelis[b]

Polypyrrole (PPy), like other conducting polymers, has a broad absorption band in the near infrared (NIR) with no evidence of fluorescence emission. We describe the preparation of PPy–EVA blends as potential hot-melt adhesives that can be activated by irradiation with NIR light. The PPy content needed to act as a thermal transducer of NIR radiation is much lower than that needed for conductivity. Blends were prepared in two ways: by blending sterically-stabilized 50 nm diameter PPy particles in water with a dispersion of 800 nm diameter ethylene–vinyl acetate copolymer (EVA) particles, and by synthesizing PPy-coated EVA core-shell particles by precipitation polymerization in water. The PPy nanoparticles and the PPy-coated EVA core-shell particles could be purified by sedimentation followed by redispersion in water to remove Fe salts. Films prepared from these particles, containing 0.1–0.5 wt% PPy, showed a strong NIR absorbance in the range of our spectrometer (700–1100 nm) with a weaker absorbance in the visible region. Photothermal radiometry (PTR) measurements indicate that these blends show good promise as potential NIR-activated adhesives, which are essentially transparent to the eye.

Introduction

In this paper we describe the preparation of processable thermoplastic polymer–PPy composites designed for applications in which the conductivity of the composite is not important. Instead, we take advantage of the broad absorption band of PPy in the NIR range of wavelengths (800–1500 nm). Composites containing PPy will absorb NIR radiation and convert the energy of the radiation into heat. In this way, one can use NIR light as an energy source to provide local heating in applications such as hot-melt adhesives. To put our work into context, we begin with a brief review of PPy composites designed as processable conductive media.

Conducting polymers themselves are of considerable interest because of their widespread applications, such as rechargeable batteries,[1–3] electronic and optical devices,[1,4] electrochromic displays,[1] sensors,[1,5] functional electrodes,[1] corrosion prevention materials,[1] and electrostatic discharge and electromagnetic interference shielding materials.[6] However, most conducting polymers have at least one of the following undesirable characteristics: (1) environmental instability, (2) their intractability, and (3) poor physical properties. Among conducting polymers, PPy is one of the materials most investigated because of its good electrical conductivity, redox properties, thermal and environmental stability. PPy has been prepared either by chemical[7] or electrochemical oxidative polymerization.[8] The electrochemical polymerization of pyrrole (Py) produces free-standing conducting films with conductivities as high as 10^2 S cm^{-1}.[9] On the other hand, the chemical polymerization method produces an insoluble black powder with a conductivity ranging from 10^{-15} to 10^1 S cm^{-1}, depending on the specific preparative conditions.[10] However, both the electrochemically generated polypyrrole (PPy) films and the chemically prepared PPy powders are difficult to process, limiting their potential for applications.

Great efforts have been made to improve PPy processability, and various approaches have been developed. One approach was to use a copolymerization method,[11,12] in which graft, block or random conductive copolymers are prepared. The other approach was to prepare composites,[13–17] in which a conductive polymer was incorporated into an insulating polymer matrix.

Another approach to improve the processability of PPy is to synthesize PPy in the form of latex particles. Kanazawa[18] carried out the precipitation polymerizations of Py in a variety of non-aqueous but semi-polar solvents, such as acetonitrile. Pron et al.[19] described an aqueous (aqueous/ethanol)-based synthesis, using FeCl$_3$ as initiator, which was subsequently used by Bjorklund and Liedberg[20] and by Armes and co-workers[21,22] to obtain colloidal forms of PPy. Bjorklund and Liedberg[20] carried out the polymerization of Py in aqueous solutions of methylcellulose. About the same time, Armes and Vincent[21] developed a colloidally stable latex of PPy particles by using steric stabilizers. Two types of steric stabilizers were found to be effective: poly(vinylpyrrolidone) (PVP) and poly(vinyl alcohol-co-acetate) (PVA).

In recent years, research interest in this area has been focused on the synthesis of core-shell PPy particles with various polymers as either the core or shell. Li and Kumacheva[23] carried out experiments to fabricate PPy

[a]Department of Chemistry, University of Toronto, 80 St George Street, Toronto, Ontario, Canada, M5S 3H6
E-mail: mwinnik@chem.utoronto.ca
[b]Department of Mechanical & Industrial Engineering, University of Toronto, Toronto, Ontario, Canada M5S 3G8

core-shell particles with PPy as the core and acrylic polymers as the shell. Jang and Oh[24] reported the preparation of PPy–poly(methyl methacrylate) (PMMA) core-shell nanospheres with diameters of several tens of nanometers by a two-step microemulsion polymerization. Other research efforts focused on the preparation of core-shell PPy particles with various polymers as the core and a PPy layer as the shell. In the early 1990s, Wiersma *et al.*[25,26] at DSM Research demonstrated that sterically-stabilized latex particles can be successfully coated with an outer layer of PPy (or polyaniline) in aqueous media to form conducting polymer composite latexes which exhibit good colloidal stability. These workers emphasized that using a non-ionic polymeric stabilizer such as poly(ethylene oxide) in these syntheses is critical for producing stable colloidal dispersions at high Fe^{3+} concentrations: all control experiments carried out in the absence of such non-ionic stabilizers resulted in macroscopic precipitation.[25] They coated a thin layer of PPy onto various low T_g polymer latexes of sub-micrometer dimensions (diameters ranging from 50 to 500 nm). The core polymer investigated up to date consisted of polyurethane, poly(vinyl acetate) or alkyd resins.

In addition to their conductivity, conducting polymers have another property of interest. These polymers have a broad absorption band in the NIR region. Reports in the literature show that many research groups monitor the UV-Vis-NIR spectra of their samples and use the presence of the NIR absorption as an indication that the polymer has been doped to the conducting state. To the best of our knowledge this NIR absorption has not previously been the specific property incorporated into any technological applications. There are two features of these spectra of interest to us. One is the broadband absorbance in the NIR. The other is the weaker absorbance in the visible range of wavelengths. We envision applications in which small amounts of conducting polymers are incorporated into polymer matrices as light-to-heat thermal transducers. In this way, for example, one could produce hot-melt adhesives that could be heated by exposure to a broadband irradiation source such as a halogen lamp or heated locally with a diode laser emitting in the NIR. If the quantity of conducting polymer present in the composite is sufficiently small (and well below the percolation threshold needed for conductivity) then the polymer film might have such a low absorbance of visible light as to be transparent to the eye.

In this paper we consider composites containing low levels of PPy in which the host polymer has useful hot-melt adhesive properties. We focus on an ethylene–vinyl acetate copolymer (EVA, available as an aqueous dispersion) containing 20 wt% vinyl acetate. We are interested both in blend films formed from a mixture of this latex with a colloidal solution of PPy nanoparticles and in core-shell particles in which the core polymer is EVA. While we found no previous literature describing the synthesis of EVA–PPy core-shell latex particles, the DSM Research approach appears to work well with the sterically-stabilized EVA latex that we employed. In addition to characterizing the optical properties of these films, we report photothermal radiometry (PTR) measurements that monitor quantitatively the thermal response of the polymers to NIR radiation.

Experimental

Materials

Pyrrole (Py) (98%), $FeCl_3$ (97%) and poly(vinyl alcohol) (PVOH, 87–89% hydrolyzed, M_w 85 000–146 000) were purchased from Sigma-Aldrich and used as received.

Aqueous EVA dispersion (DUR-O-SET, E200, poly(vinyl alcohol)-stabilized poly(ethylene–vinyl acetate) (E : VAc 8 : 2 w/w, solids 56.6 wt%, pH 4.5, T_g 0 °C) was provided by National Starch and Chemical Co., and was used as received. De-ionized water obtained from a MilliQ™ water purification system was used in all experiments.

Synthesis of polypyrrole (PPy)-coated EVA core-shell latex

This preparation was based on a modification of the DSM approach.[26] A solution of Py (0.89 g in 44 g water) was mixed with a sterically-stabilized EVA latex (13 g, DUR-O-SET, E220) under stirring for 10 min. Subsequently, $FeCl_3$ (3.7 g) dissolved in water (210 g) was added slowly to the above mixture at room temperature. The reaction was allowed to proceed for 24 h. The mixture was filtered through a copper sieve (150 micron mesh size).

Synthesis of polypyrrole (PPy) nanoparticles

A solution of Py (0.87 g in 20 g water) was mixed with PVOH (0.87 g) dissolved in 30 g water) under stirring for 10 min. Subsequently, $FeCl_3$ (3.7 g) dissolved in water (210 g) was added slowly to the mixture at room temperature. The reaction proceeded for 24 h. The mixture was filtered through a copper sieve (150 micron mesh size).

Latex film preparation

Thin latex films were cast from EVA latex (DUR-O-SET, E220) blended with PPy-coated EVA core-shell latex or PPy nanoparticles with the help of a drawdown bar.

Electron microscopy measurements

High resolution scanning electron microscopy (SEM) images of cast films were obtained with a Hitachi S-5200, operated at 0.7 kV and 10 μA.

Particle samples were examined by scanning transmission electron microscopy (STEM) with a Hitachi HD-2000 instrument equipped with an Energy Dispersive X-Ray (EDX) Spectroscopy system, operated at 200 kV and 30 μA. PPy-coated EVA core-shell latex and PPy latex were diluted to about 0.01 wt% solids with water. One drop of a solution was deposited directly onto a carbon-coated copper grid supported on a Formvar film. Water was allowed to evaporate at ambient pressure and temperature. Some samples of PPy-coated EVA particles were characterized by EDX. Inca software (Oxford Instruments Plc.) was used to obtain the elemental profile across the image.

UV-Vis-NIR spectroscopy

A Perkin Elmer, Lambda 25 spectrometer was used to measure the absorbance of the cast films in the wavelength range of 300–1100 nm.

Elemental analysis

The PPy content of some samples was determined in-house by C/H/N elemental analysis using a 2400 CHN Elemental Analyzer (Perkin Elmer). Fe content was measured by using a digestion method. A dried sample was accurately weighted on a Sartorius Analytical balance (five digits), and treated with a mixture of concentrated nitric acid and sulfuric acid (volume ratio 3 : 8) and left overnight. The sample was then processed in an Anton-Paar Microwave Digestion system set at 50% (500 W) strength for 30 min. Fe analysis was accomplished by ICP analysis (Perkin Elmer Optima 3000DV). Four standard samples of iron solutions (0.1, 1, 10 and 100 ppm) were used for calibration with a mean regression of more than 0.99995.

Photothermal radiometry (PTR) experiments

Laser infrared PTR measurements were carried out as described in ref 27. The experimental setup is presented in Fig. 1. A semiconductor laser emitting at 830 nm (maximum power 100 mW, Sanyo DL-7032-001) was used as a source of the PTR signal. A diode laser driver (ThorLabs GmbH, Model LDC210) was used for the laser and was triggered by the built-in function generator of the lock-in amplifier (EG&G Instruments, Model 7265 DSP), modulating the laser current harmonically. The lock-in amplifier was controlled by a computer *via* RS-232 ports. The laser beam was focused on the sample with a high-performance lens (Gradium GPX085, focal length: 200 mm) to a spot size of 121 $\pm$ 8 μm. The modulated PTR signal from the sample was collected and focused by two off-axis paraboloidal mirrors (Melles Griot 02POA017, rhodium-coated) onto a mercury cadmium telluride (HgCdTe or MCT) detector (EG&G Judson). Before being sent to the lock-in amplifier, the PTR signal was amplified by a preamplifier (EG&G Judson PA-101). The polymer films were attached to a plastic ring and glued to a Lego-brick in order to make them suitable for positional adjustment using a micrometer stage.
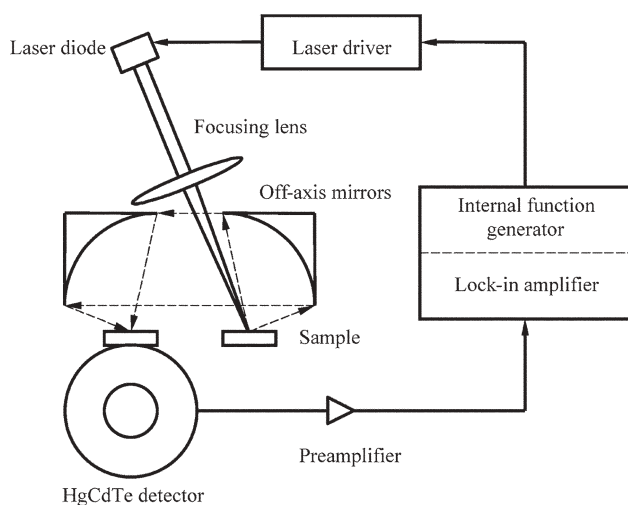
Results and discussion

The synthesis of PPy nanoparticles and PPy–EVA composite particles

We envisioned two approaches to preparing PPy–EVA films from waterborne precursors. First, one could prepare a colloidal dispersion of PPy nanoparticles and blend it with a low T_g EVA dispersion. Films formed from this mixture should contain the PPy nanoparticles embedded in the EVA matrix. Alternatively, one could synthesize the PPy nanoparticles in the presence of an EVA latex. This approach, which follows the DSM methodology, should lead to the formation of core-shell structures consisting of EVA particles coated with a layer of PPy. For the relatively low amounts of PPy that we anticipate would be needed for NIR-activated adhesives, the core-shell materials could be diluted with additional EVA latex and then used to prepare the films. To test these ideas, we employed a commercial EVA latex (DUR-O-SET E220), which contains approximately 80% ethylene by weight and consists of a broad distribution of particle sizes ranging from *ca.* 300 to 900 nm in diameter. Differential scanning calorimetry (DSC) measurements show that the polymer has a T_g of 0 °C and no discernable melting transition for temperatures up to 150 °C. The latex forms films spontaneously upon drying. These films are transparent, tack-free, and for thicknesses of the order of 0.5–1 mm have reasonable mechanical integrity.

To prepare PPy nanoparticles, we treated an aqueous solution of pyrrole containing poly(vinyl alcohol) (PVOH) with $FeCl_3$. This led to the formation of very uniform PVOH-stabilized PPy particles with a mean diameter of *ca.* 50 nm. A scanning microscopy (SEM) image of these particles is shown in Fig. 2A. Iron salts (primarily $FeCl_2$) are an unwanted by-product in these dispersions. In order to minimize the iron content in the product, particles were sedimented by centrifugation at 14 000 rpm for one hour. The supernatant was removed, and the sediment was redispersed in water. This

Fig. 1 Schematic diagram of the experimental setup for PRT measurements.
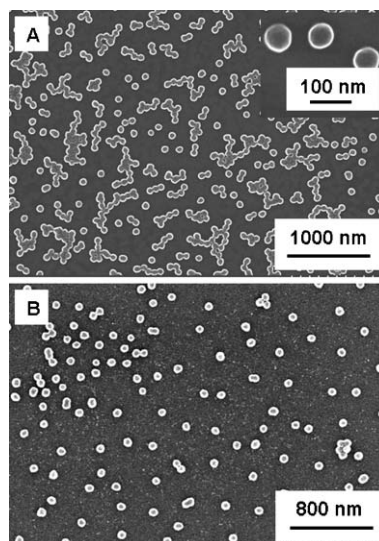
Fig. 2 SEM images of PVOH-stabilized PPy particles: (A) before purification, and (B) after three centrifugation–redispersion cycles.

This journal is © The Royal Society of Chemistry 2007

J. Mater. Chem., 2007, **17**, 4309–4315 | 4311

procedure could be repeated. As we show below, three successive sedimentation–redispersion steps reduce the Fe content of the samples by more than 90%. The upper and lower images in Fig. 2 compare the morphology of the PPy nanoparticles before and after the removal of iron salts from the dispersion. The important point is that one can reduce the Fe content of the PPy nanoparticles while maintaining their colloidal stability.

The DUR-O-SET EVA latex is a PVOH-stabilized dispersion that contains excess PVOH. When the oxidative polymerization of pyrrole with $FeCl_3$ was carried out *in situ* in the presence of this latex, we obtained a mixture of PPy-coated EVA particles and individual PPy nanoparticles that resemble those shown in Fig. 2. The chemical yield of PPy, as determined by elemental analysis for nitrogen, was sensitive to the molar ratio of $FeCl_3$ to Py. When this ratio was 2 : 1, we obtained an 84% yield of PPy, but when a 1 : 1 ratio was employed, we obtained only a 41% yield. The morphology of the product obtained can be inferred by comparing the SEM image of the reaction product in Fig. 3B with that of the EVA latex particles themselves in Fig. 3A. Particularly from the inset in Fig. 3B, which provides a magnified image of one of the composite particles, one can see that the reaction has led to the formation of composite EVA particles whose surfaces are decorated with PPy nanoparticles.

For these samples, as well, excess iron salts were removed by three successive sedimentation–redispersion cycles in which the centrifugation was carried out for 30 min at 13 000 rpm. The Fe content of the core-shell particle sample, before and after purification, was measured by ICP-AES following sample

digestion as described in the Experimental section. For the sample prepared with a 2 : 1 ratio of $FeCl_3$–Py, the Fe content was 9.06 wt% (corresponding to 20.6 wt% $FeCl_2$), *versus* 0.028 wt% Fe (corresponding to 0.06 wt% $FeCl_2$) for the sample purified by three cycles of sedimentation and redispersion. This reduction in Fe content was also confirmed by EDX analysis. This purification procedure led to the loss of some of the small PPy particles in the sample. The best indication of the reduction in the number of small particles is the decrease in the ratio of small to large particles seen in the comparison of the SEM images in Fig. 3B (before purification) and Fig. 3C (after purification). Again we found that the Fe content could be dramatically reduced without interfering with the colloidal stability of the particles.

**Latex blends, their films and their NIR absorption spectra**

In this section we describe films formed from blends of the EVA latex with the PPy-coated EVA core-shell particles and with the PVOH-stabilized small PPy particles. Blend films containing PPy or core-shell particles were prepared by mixing the aqueous dispersions and then casting films using a drawdown bar. Examples of blend films prepared with the core-shell particles are shown in Fig. 4 in which we compare in (A) a film obtained from a blend with unpurified PPy-coated EVA latex, with a film in (B) prepared from a purified sample of PPy-coated EVA latex. Both films contained 0.5 wt% PPy. In (A) one can see two types of features characteristic of the
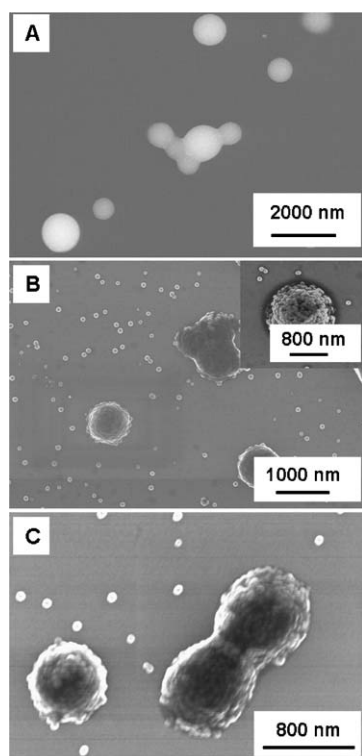
Fig. 3 SEM images of PPy-coated EVA particles: (A) EVA particles, (B) before purification, and (C) after three centrifugation–redispersion cycles.
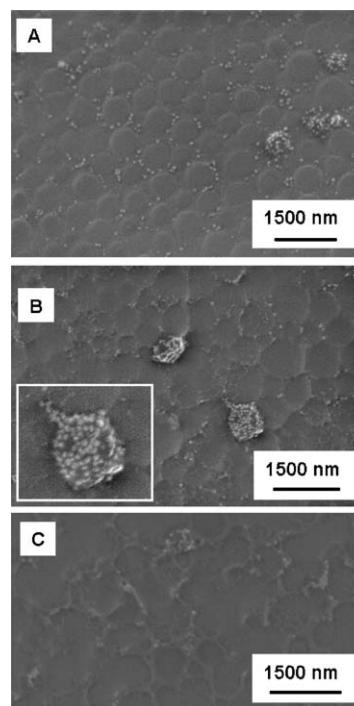
Fig. 4 SEM images of cast films from a blend of EVA latex (DUR-O-Set E200) plus PPy-coated EVA core-shell latex particles. (A) EVA latex plus unpurified PPy-coated EVA latex. (B) EVA latex plus PPy-coated EVA latex purified by three centrifugation–redispersion cycles. Both samples contain 0.5 wt% PPy. The inset in (B) is a magnified image of one of the larger objects which form part of the film seen in (B). (C) A sample corresponding to film B after annealing at 120 °C for 10 min.
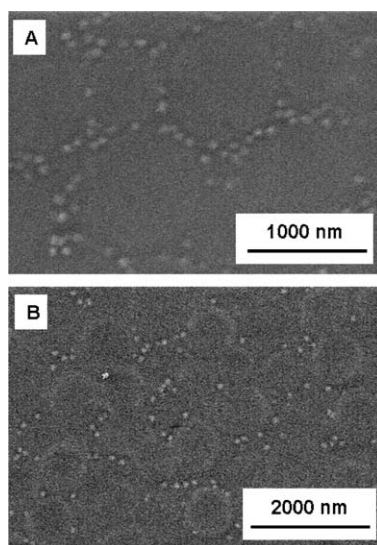
Fig. 5 SEM images of films formed from blends of EVA latex with a dispersion of the PPy nanoparticles shown in Fig. 2: (A) EVA latex plus unpurified PPy nanoparticles, and (B) EVA latex plus PPy nanoparticles purified by three centrifugation–redispersion cycles. Both films contain 0.5 wt% PPy.

PPy component: small PPy particles confined to the boundary regions between the larger EVA particles, and core-shell particles consisting of EVA particles coated with PPy nanoparticles. In (B), one can see the outline of deformed EVA particles as well as two core-shell particles that appear largely undeformed in the film. A magnified image of one of the core-shell particles is shown in the inset in this figure. One can also see small isolated PPy particles, fewer in number than in (A), a consequence of the purification procedure used to remove excess Fe^{2+} from this core-shell sample. As a test of the types of morphology changes that might be expected for a sample employed as a hot-melt adhesive, a film with the composition corresponding to that in Fig. 4B was annealed for 10 min at 120 °C. An SEM image of this film is shown in Fig. 4C. While there is evidence for further coalescence and some polymer flow upon heating, the overall morphology is not much different from that of the as-prepared film.

Fig. 5 presents SEM images of films cast from blends of EVA latex with the PVOH-stabilized PPy nanoparticles, comparing the blend formed from the unpurified PPy particle dispersion in (A) with a film formed from the purified PPy particle dispersion in (B). Both images show contours of objects with a diameter of about 800 nm, with the 50 nm PPy particles confined to these contours. This type of packing is typical for blends of large soft latex particles with small hard particles.[28] Both films contain 0.5 wt% PPy, and there is not much difference to be seen in the images. These results demonstrate that PPy particles stabilized by PVOH have a good dispersibility in EVA latex blend films. The presence of the iron salts from the unpurified PPy sample does not appear to affect any easily observable aspect of film formation.

These various blend films exhibit an absorption in the NIR spectrum consistent with the conducting form of PPy. Three examples are shown in Fig. 6. The curves labeled **2:1p** and **2:1u** refer to films prepared with the purified and unpurified
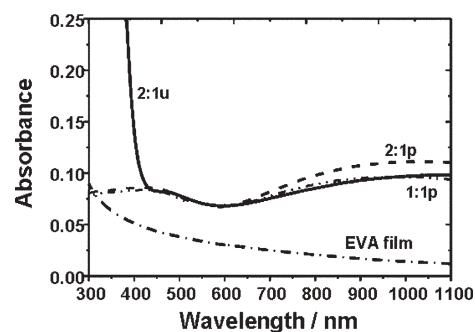
Fig. 6 NIR absorption of 6 μm thick EVA/(EVA–PPy core-shell) blend films containing 0.5 wt% PPy: **u** and **p** indicate unpurified and purified EVA–PPy core-shell samples, respectively; **2:1** and **1:1** indicate the molar ratio of Fe^{3+}–Py used in the synthesis of the core-shell particles. The bottom curve is the absorbance of a film prepared from the EVA latex itself.

EVA–PPy core-shell particles respectively in which the particles were synthesized with a 2 : 1 molar ratio of Fe^{3+} to Py. The curve labeled **1:1p** refers to a film containing the purified core-shell particles prepared with a 1 : 1 molar ratio of Fe^{3+} to Py. All films contain 0.5 wt% PPy. They all have a similar and significant absorbance in the NIR region, between 700 and 1100 nm, and a weaker absorbance between 450 and 650 nm. The unpurified sample shows a much stronger absorbance between 350 and 450 nm, a consequence of Fe salts remaining in the sample. The similarity of the spectra seen for the **2:1p** and **1:1p** samples is interesting because in ref. 16, Ruckenstein and Yang reported a higher electrical conductivity for PPy–EVA composites prepared with a 2 : 1 rather than a 1 : 1 Fe^{3+}–Py ratio.[29]

Photothermal radiometry measurements

PTR experiments detect the infrared radiation emitted from a sample when intensity-modulated laser light impinges on its surface. The resulting infrared flux depends on the optical and thermal properties of the sample, such as thermal diffusivity and the optical absorption coefficient. The spectrally integrated radiation heat flux W at the sample–air interface can be written as:

$$W = \varepsilon \sigma_{SB} T^4 \qquad (1)$$

where σ_{SB} is the Stefan–Boltzmann constant and ε is the emissivity of a sample. The temperature of the surface T includes a small oscillating component at frequency f. In other words, the temperature is the sum of dc and ac components. The ac temperature is much smaller than the dc temperature, so the temperature expression can be linearized as follows:

$$T(t) = T_{dc} + T_{ac} \exp(i2\pi ft)$$
$$T^4(t) = [T_{dc} + T_{ac} \exp(i2\pi ft)]^4 \approx T_{dc}^4 + 4T_{dc}^3 T_{ac} \exp(i2\pi ft) \qquad (2)$$

The ac component of infrared flux at the sample front surface becomes:

$$W_{ac}(\alpha,\beta,f) \approx 4\varepsilon \sigma_{SB} T_{dc}^3 T_{ac}(\alpha,\beta,f) \qquad (3)$$

This journal is © The Royal Society of Chemistry 2007

*J. Mater. Chem.*, 2007, **17**, 4309–4315 | 4313

where the oscillating temperature depends on the thermal properties of a sample and modulation frequency.[30] Here α is the thermal diffusivity of the sample, β is the absorption coefficient.

An example of the PTR analysis of a set of PPy-containing EVA (Elvax 210) films is presented in Fig. 7. These films were cast from EVA and PPy–EVA core-shell latex blends as described for the samples in Fig. 4. In (A) we plot the measured absorbances of the films at the laser irradiation wavelength (830 nm). As expected from Beer's Law, the absorbance increases linearly with PPy concentration. In (B) we plot the PTR signal, represented here by the amplitude of the oscillating infrared flux. The signal at a fixed frequency and fixed position was measured five consecutive times, and the results were averaged. The signal for the film without PPy is very weak. The sample with 0.01 wt% PPy exhibited a signal amplitude about two orders of magnitude higher than that of the EVA film without PPy. These large increases in the PTR signal are seen because the optical absorption in the PPy-labeled samples becomes very significant, and the amplitude of the thermal wave at the excited spot, the result of optical-to-thermal (non-radiative) energy conversion, rises substantially. The samples with higher concentrations of PPy accordingly exhibit higher signals. Unlike the absorption coefficient dependence on PPy concentration, the PTR signals are non-linear in the absorption coefficient of the polymer at the excitation wavelength and they tend to saturate at high PPy concentrations, a phenomenon known as photothermal saturation.[31]

We also carried out experiments in which we monitored the variation of the PTR response with position across the film. An example is represented in Fig. 8, where (A) shows the response of a blank EVA film (DUR-O-Set E200) without PPy and (B) shows the much higher response for a film (the same film shown in Fig. 4B) containing 0.5 wt% PPy. Note that the amplitude of the PTR signal in (A) is multiplied by a factor of 10^5. The peaks and valleys in these plots are due to surface imperfections. What is interesting in the comparison between Fig. 8A and 8B is the decrease in the signal for the film with
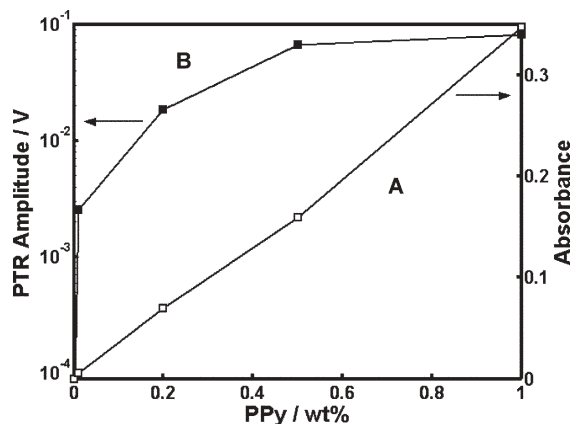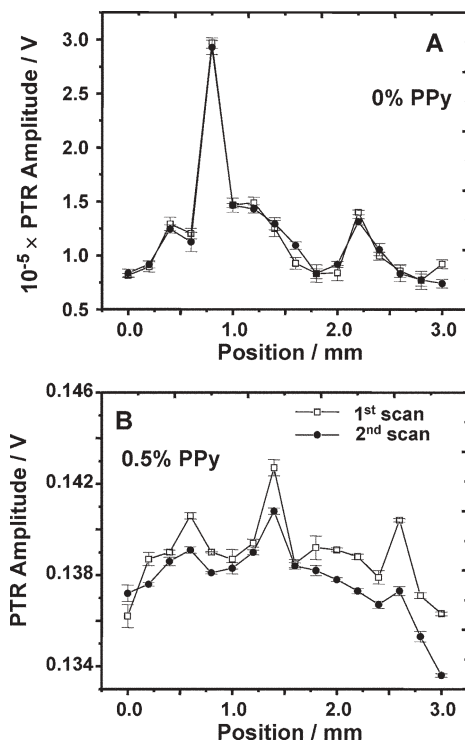
Fig. 8 Comparison of the PTR response of (A) an EVA film (DUR-O-Set E200, 0.8 mm thick), and (B) a similar film containing 0.5 wt% PPy. Line scans at a frequency f = 20 Hz. Each sample was scanned twice along the same line.

PPy when the surface is scanned a second time along the same line. After the first scan, there is also a 'scar' on the film indicating damage to the film along the line traced by the laser. This change is in contrast with the reproducibility of the signal for the PPy-free film. The change in signal for the film with PPy corresponds to a line thermally etched into the film through laser melting and resolidification as a consequence of NIR irradiation. These results provide compelling evidence for the ability of the PPy in the film to convert NIR excitation into heat very efficiently.

Summary

We polymerized Py in water with $FeCl_3$ in the presence of EVA latex particles sterically stabilized with PVOH. This led to a dispersion of EVA particles coated with small (50 nm diameter) PPy particles as well as a significant population of similarly sized free PPy particles. The PPy particles themselves could be prepared by precipitation polymerization of Py in the presence of PVOH. Both of these sterically-stabilized dispersions could be purified to remove Fe^{2+} in the samples by sedimentation followed by redispersion in water.

Latex blend films were prepared by mixing either of the sterically-stabilized PPy dispersions with excess EVA latex and then casting films on a transparent substrate. These films, containing typically 0.5 wt% PPy, exhibited a significant absorbance in the region of 700–1100 nm, and a weaker absorbance in the visible region. Nearly transparent films were excited by light from a laser at 830 nm and monitored for their photothermal response. The light absorbance due to the

Fig. 7 EVA films (DUR-O-Set E200, 800 nm thick) containing different amounts of PPy: (A) absorbance at 830 nm *vs.* concentration of PPy, and (B) PTR amplitude at a frequency f = 20 Hz. The point at the lowest non-zero PPy concentration appears at 10 ppm (0.01 wt%) along the *x*-axis.

presence of the PPy was very effective at generating heat in the samples. Even very thin films showed not only strong transduction of light energy into heat, but they also showed signs of surface melting in the regions exposed to the laser.

Acknowledgements

References

1 X. Li, M. Huang, W. Duan and Y. Yang, *Chem. Rev.*, 2002, **102**(9), 2925–3030.

2 J. Y. Lee, L. H. Ong and G. K. Chuah, *J. Appl. Electrochem.*, 1992, **22**(8), 738–742.

3 D. K. Moon, A. B. Padias, H. K. Hall, T. Huntoon and P. D. Calvert, *Macromolecules*, 1995, **28**(18), 6205–6210.

4 B. W. Maynor, S. F. Filocamo, M. W. Grinstaff and J. Liu, *J. Am. Chem. Soc.*, 2002, **124**(4), 522–523.

5 A. Talaie, J. Y. Lee, J. Jang, J. A. Romagnoli, T. Taguchi and E. Maeder, *Thin Solid Films*, 2000, **363**(1–2), 163–166.

6 J. Y. Zhang, J. Li, X. H. Wang, X. B. Jing and F. S. Wang, *J. Funct. Polym.*, 1999, **12**, 350–356 (in Chinese).

7 F. Hautiere-Cristofini, D. Kuffer and L. T. Yu, *C. R. Acad. Sci. Paris, Ser. C*, 1973, **277**(24), 1323–1326; K. C. Khulbe and R. S. Marn, *J. Polym. Sci.: Polym. Chem. Ed.*, 1982, **20**(4), 1089–1095; M. M. Castillo-Ortega and M. B. Inoue, *Synth. Met.*, 1989, **28**, C65.

8 A. F. Diaz, K. Kanazawa and G. P. Gardini, *J. Chem. Soc., Chem. Commun.*, 1979, 635–636; R. J. Waltman and J. Bargon, *Can. J. Chem.*, 1986, **64**(1), 76–95; G. B. Street, T. C. Clarke, M. Krounbi, K. K. Kanazawa, V. Y. Lee, P. Pfluger, J. C. Scott and G. Weiser, *Mol. Cryst. Liq. Cryst.*, 1982, **83**(1–4), 1285–1296.

9 K. K. Kanazawa, A. F. Diaz, R. H. Geiss, W. D. Gill, J. F. Kwak, J. A. Logan, J. F. Rabolt and G. B. Street, *J. Chem. Soc., Chem. Commun.*, 1979, 854–855.

10 R. E. Myers, *J. Electron. Mater.*, 1986, **15**(2), 61–69.

11 A. I. Nazzal and G. B. Street, *J. Chem. Soc., Chem. Commun.*, 1985, 375–376.

12 R. W. Gumbs, *Synth. Met.*, 1994, **64**(1), 27–31.

13 E. Ruckenstein and J. S. Park, *J. Appl. Polym. Sci.*, 1991, **42**(4), 925–934.

14 Y. Sun and E. Ruckenstein, *Synth. Met.*, 1995, **72**(3), 261–267.

15 E. Ruckenstein and L. Hong, *Synth. Met.*, 1994, **66**(3), 249–256.

16 E. Ruckenstein and S. Yang, *Polymer*, 1993, **34**(22), 4655–4660.

17 S. Yang and E. Ruckenstein, *Synth. Met.*, 1993, **60**(30), 249–254.

18 K. K. Kanazawa, *Synth. Met.*, 1981, **4**(2), 119–130.

19 A. Pron, Z. Kucharski, C. Budrowski, M. Zagorska, S. Krichene, J. Suwalski, G. Dehe and S. Lefrant, *J. Chem. Phys.*, 1985, **83**(11), 5923–5927.

20 R. B. Bjorklund and B. Liedberg, *J. Chem. Soc., Chem. Commun.*, 1986, 1293–1295.

21 S. P. Armes and B. Vincent, *J. Chem. Soc., Chem. Commun.*, 1987, 288–290.

22 S. P. Armes, J. F. Miller and B. Vincent, *J. Colloid Interface Sci.*, 1987, **118**(2), 410–416.

23 H. Li and E. Kumacheva, *Colloid Polym. Sci.*, 2003, **281**(1), 1–9.

24 J. Jang and J. K. Oh, *Adv. Func. Mater*, 2005, **15**(3), 494–502.

25 A. E. Wiersma and L. M. A. vd Steeg, *Eur. Pat.*, 1993, 589,529; A. E. Wiersma and L. M. A. vd Steeg, *US Pat.*, 1995, 5,415,893.

26 A. E. Wiersma, L. M. A. vd Steeg and T. J. M. Jongeling, *Synth. Met.*, 1995, **71**(1–3), 2269–2270.

27 R. J. Jeon, C. Han, A. Mandelis, V. Sanchez and S. H. Abrams, *Caries Res.*, 2004, **38**(6), 497–513.

28 S. T. Eckersley and B. J. Helmer, *J. Coat. Technol.*, 1997, **69**(864), 97–107.

29 Using equipment in the laboratory of Professor Al-Amin Dhirani, we measured the conductivity of films cast from the **2:1p** sample of PPy-coated EVA latex using the standard four-point technique. One sample film containing 8 wt% PPy had a conductivity of 2.02 S m^{-1}, consistent with the value of 3.0 S m^{-1} for the PPy–PEMA composite with 10 wt% PPy reported by Ruckenstein and Yang in ref. 16.

30 A. Mandelis, *Diffusion-Wave Fields: Mathematical Methods and Green Functions*, Springer-Verlag, New York, 2001.

31 A. Rosencwaig and A. Gersho, *J. Appl. Phys.*, 1976, **47**(1), 64–69; see also A. Mandelis in ref. 30, p.105.